

# Scalar Mesons $a_0(1450)$ and $\sigma(600)$ from Lattice QCD

N. Mathur<sup>a</sup>, A. Alexandru<sup>b</sup>, Y. Chen<sup>c</sup>, S.J. Dong<sup>b</sup>, T. Draper<sup>b</sup>,  
I. Horváth<sup>b</sup>, F.X. Lee<sup>d</sup>, K.F. Liu<sup>b</sup>, S. Tamhankar<sup>e</sup>, and J.B. Zhang<sup>f</sup>

<sup>a</sup>Jefferson Lab, 12000 Jefferson Avenue, Newport News, VA 23606

<sup>b</sup>Dept. of Physics and Astronomy, University of Kentucky, Lexington, KY 40506

<sup>c</sup>Institute of High Energy Physics, Beijing 100039, China

<sup>d</sup>Dept. of Physics, George Washington University, Washington, DC 20052

<sup>e</sup>Dept. of Physics, Hamline University, St. Paul, MN 55104

<sup>f</sup>Dept. of Physics, Zhejiang University, Hangzhou, Zhejiang 310027, China

We study the  $a_0$  and  $\sigma$  mesons with the overlap fermion in the chiral regime with the pion mass as low as 182 MeV in the quenched approximation. After the  $\eta'\pi$  ghost states are separated, we find the  $a_0$  mass with  $q\bar{q}$  interpolation field to be almost independent of the quark mass in the region below the strange quark mass. The chirally extrapolated results are consistent with  $a_0(1450)$  being the  $u\bar{d}$  meson and  $K_0^*(1430)$  being the  $u\bar{s}$  meson with calculated masses at  $1.42 \pm 0.13$  GeV and  $1.41 \pm 0.12$  GeV respectively. We also calculate the scalar mesonium with a tetraquark interpolation field. In addition to the two pion scattering states, we find a state at  $\sim 550$  MeV. Through the study of volume dependence, we confirm that this state is a one-particle state, in contrast to the two-pion scattering states. This suggests that the observed state is a tetraquark mesonium which is quite possibly the  $\sigma(600)$  meson.

PACS numbers: 12.38.Gc, 14.20.Gk, 11.15.Ha

## I. INTRODUCTION

Unlike pseudoscalar, vector, and tensor mesons, the scalar mesons are not well known in terms of their  $SU(3)$  classification, the particle content of their composition, or their spectroscopy. Part of the problem is that there are too many experimental candidates for the  $q\bar{q}$  nonet. Fig. 1 shows the current experimentally known scalar mesons whose number more than doubles that of a nonet. One viable solution is that low-lying scalars, such as the  $\sigma(600)$ ,  $a_0(980)$  and  $f_0(980)$  are tetraquark mesoniums whose classification and spectroscopy have been studied in the MIT bag model [1] and the potential model [2]. Another suggestion is that  $a_0(980)$  and  $f_0(980)$  are  $K\bar{K}$  molecular states [3]. Other candidates for tetraquark mesoniums include vector mesons pairs produced in  $\gamma\gamma$  reactions [4] and hadronic productions [5] and the recently discovered charmed narrow resonances [6].

Under the supposition that  $a_0(980)$  and  $f_0(980)$  are tetraquark mesoniums on account of the fact that they are favored by spectroscopy studies [1, 2], small two-photon decay widths [7], and the pattern of  $\phi$  and  $J/\Psi$  decays [8], the question remains: where is the isovector scalar  $q\bar{q}$  state? From Fig. 1, we see that one candidate is  $a_0(1450)$ . However, in the conventional wisdom of the quark model, its mass is too high. Not only is it higher than  $a_2(1320)$  and  $a_1(1230)$ , in contrast to the spin-orbit splitting pattern in charmonium; it is even slightly higher than  $K_0^*(1430)$  which contains a strange quark and is believed to be the  $s\bar{u}$  or  $s\bar{d}$  meson in practically all

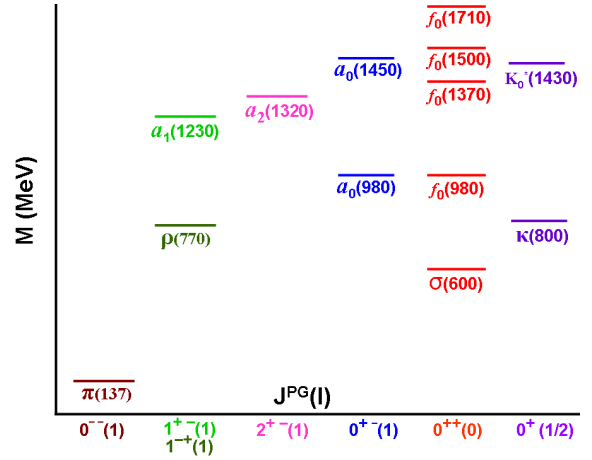


FIG. 1: Spectrum of scalar mesons together with  $\pi$ ,  $\rho$ ,  $a_1$  and  $a_2$  mesons.

the models [9]. According to the quark counting rule, mesons and baryons made up of strange quarks are expected to lie higher than their counterparts with  $u/d$  quarks. Notwithstanding the success of the quark potential model in describing charm and bottom hadrons, its applicability to light hadrons with  $SU(6)$  symmetry has been questioned, since chiral symmetry plays an essential role [10, 11] in light hadron dynamics. Might it be that the scalar  $q\bar{q}$  meson is yet another challenge to the  $SU(6)$  quark model's delineation of light hadrons?

Lattice QCD is perhaps the most desirable tool to adjudicate the theoretical controversy surrounding the issue and to reveal the nature of the scalar

mesons. In fact, there have been several calculations to study the  $a_0$  meson with the  $\bar{\psi}\psi$  interpolation field in the quenched approximation [12, 13, 14] and with dynamical fermions [15, 16, 17, 18, 19]. In calculations with relatively small quark masses, it is found that the  $a_0$  mass does not change much below the strange quark mass. Consequently, the chiral limit result is consistent with  $a_0(1450)$ . Furthermore, it is emphasized that the would-be  $\eta'\pi$  ghost states give negative contributions to the  $a_0$  correlator in both the quenched case [13] and the partially quenched case [16] when the quark mass is lower than the strange. Thus it is essential to take out these quenched or partially quenched artifacts before one can confidently obtain the  $a_0$  mass. In the case of  $\sigma$ , a calculation of the tetraquark mesonium with the pseudoscalar-pseudoscalar 4-quark interpolation field [20] has been performed. From the deviation of the lowest state mass from that of the expected two-pion scattering state, it was suggested [20] that a bound mesonium state is seen.

In the present work, we shall use the overlap fermion [21] to calculate  $a_0$  and the scalar tetraquark mesonium. The overlap fermion has the benefit of having exact chiral symmetry at finite lattice spacing. Since chiral symmetry plays a pivotal role in these mesons in chiral effective theories (in particular, it is concluded in the recent dispersion analysis of  $\pi\pi$  scattering that the occurrence of  $\sigma$  is on the basis of “current algebra, spontaneous symmetry breakdown, and unitarity” [22]), we believe it is desirable to adopt a fermion action which explicitly exhibits the spontaneously broken chiral symmetry at finite lattice spacing.

For the study of  $a_0$ , it is well known that there are  $\eta'\pi$  ghost states in the quenched [13, 14] and partially quenched [16] cases. These ghost states become the physical  $\eta\pi$  and  $\eta'\pi$  states in the full dynamical calculation without partial quenching. Such physical two meson states in full QCD have been seen when the quark masses are light enough [15]. Thus, in order to obtain  $a_0(1450)$  and possibly  $a_0(980)$  in the quenched approximation, one needs an algorithm which can fit multiple states including the  $\eta'\pi$  ghost states which lie lower in mass than the  $I = 1$  scalar  $q\bar{q}$  below the strange quark mass region. We have developed a sequential empirical Bayes method (SEBM) for constrained-curve fitting [23] to fit multiple states. This is based on the constrained-curve fitting of lattice data with Bayesian priors [24, 25]. In the sequential empirical Bayes method [23], one extracts the priors for the mass and spectral weight from a subset of data by fitting the two-point correlation function starting from the large time separation. First, one fits the ground state in a time window and then uses its fit-

ted mass and spectral weight as priors to fit the first excited state in an extended time window. The process is repeated until time slices are exhausted. One then does a constrained-curve fit to the rest of the data set with the extracted priors. This method has been employed to fit the Roper resonance, the radially excited nucleon, and  $S_{11}(1535)$  on top of the  $\eta'N$  ghost states [11]. It has also been used in extracting radially-excited states of 1P charmonium [26].

It turns out that, for the range of quark masses that we fitted, the 3-volume dependence (from a comparison of  $16^3 \times 28$  and  $12^3 \times 28$  lattices) of the spectral weights of the respective ghost  $\eta'N$  two-particle scattering state and the bound one-particle baryon state come out in agreement with expectation, as derived in Ref. [11, 27]. We regard this as a highly non-trivial test for the fitting method. Similarly, in the study of the pentaquark state  $\Theta^+(1540)$ , we fitted the state in addition to the  $\eta'KN$  ghost state and found from the volume dependence that it is in agreement with the  $KN$  scattering state for a large range of quark masses [27]. Through these studies, we are more confident that the fitting method is capable of fitting multiple states including the ghost states. It is of course limited by how good the data are and how many states one can fit, given the number of time slices of the lattice. We shall use this algorithm in the present study of  $a_0(1450)$  and  $\sigma(600)$ . The smallest pion we have is 182(8) MeV, which is substantially lower than most of the previous calculations of  $a_0$ ; this allows us to study the behavior of  $a_0$  with the pseudoscalar meson mass ranging from 1.3 GeV down to 182 MeV. This is important in revealing that the  $a_0$  mass is very insensitive to quark mass in the range from strange quark down to the physical  $u/d$  mass. This turns out to have significant phenomenological implications on the pattern of scalar mesons [28]. For the study of the  $\pi\pi$  mesonium with the tetraquark interpolation field on our lattice, it is crucial for the pion mass to be lower than  $\sim 300$  MeV in order to be able to disentangle the  $\pi\pi$  scattering states from the one-particle mesonium, in order to reveal the nature of the fitted states from the tetraquark correlator. Thus, for both the case of  $a_0(1450)$  and  $\sigma(600)$ , it is essential to study them in the chiral regime where  $m_\pi$  is smaller than 300 MeV.

## II. $a_0(1450)$ AND $K_0^*(1430)$ MESONS

Our calculation is based on data from  $16^3 \times 28$  and  $12^3 \times 28$  lattices with 300 quenched Iwasaki gauge configurations ( $\beta = 2.264$ ) and overlap fermions with a lattice spacing  $a = 0.200(3)$  fm determined from  $f_\pi(m_\pi)$ . This makes our lattice sizes at 3.2 fm

and 2.4 fm, respectively. We will discuss the scale determination from the Sommer scale  $r_0$  later to assess the systematic error in scale setting. A subset of these quark propagators was used to study the quenched chiral logs in pion and nucleon masses [29], the Roper and  $S_{11}$  [11], and the pentaquarks [27].

There has been a concern that lattice spacing of 0.2 fm may be too coarse for the overlap fermion and speculation that the range of the overlap Dirac operator may be as long as 4 lattice units [30]. However, direct calculation [31] at lattice spacings of 0.2, 0.17, and 0.13 fm with Iwasaki gauge action reveals that the range of the operator is comfortably small in each of these cases (one lattice unit in Euclidean distance and 2 units in “taxi driver” distance, the latter being defined as  $r_{TD} \equiv ||x - y||_1 = \sum_{\mu=1,4} |x_\mu - y_\mu|$ ) and it approaches zero toward the continuum limit. Thus, we don’t think there is an issue regarding locality of the overlap operator at 0.2 fm that we base our results on.

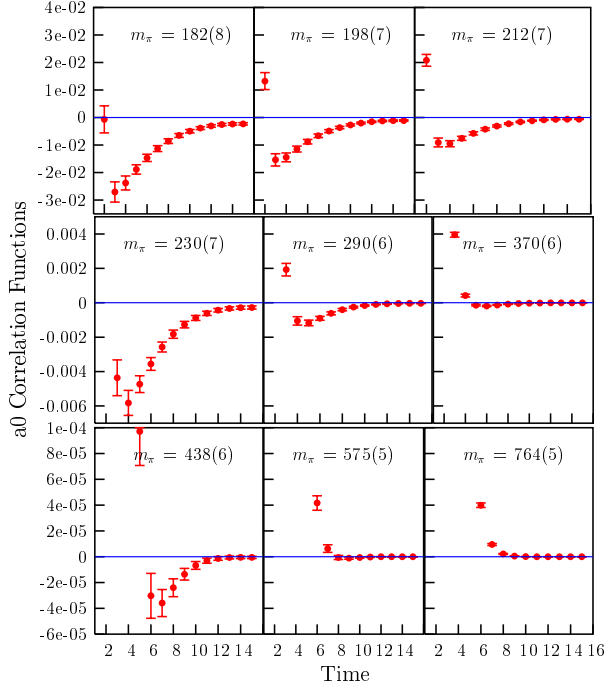


FIG. 2:  $a_0$  correlators from the  $\bar{\psi}\psi$  interpolation field for several quark masses with corresponding pion masses in MeV.

We first report results on  $a_0$  for which we use  $\bar{\psi}\psi$  as the interpolation field. Since  $a_0$  is an isovector, one only needs to calculate the correlator with the connected insertion. Shown in Fig. 2 are  $a_0$  correlators as a function of time for 9 quark cases with pion mass from  $m_\pi = 182(8)$  MeV to  $m_\pi = 764(5)$  MeV. It is seen that for pion mass lower than  $\sim 600$  MeV, the  $a_0$  correlator starts to develop a negative tail,

and it is progressively more negative at earlier time slices for smaller quark masses. This is a clear indication that at least one of the ghost  $\eta'\pi$  states, being lightest in mass, are dominating the correlator over the physical  $a_0$  at larger time slices. This has been reported in the literature for the quenched [13, 14] and partially quenched [16] calculations and the ghost contribution has been removed with the help of re-summed hairpin diagrams. The ghost  $\eta'\pi$  contribution in the  $a_0$  correlator has been studied in the chiral perturbation theory [13, 16]. The one-loop hairpin diagram gives the following contribution to the isovector scalar meson propagator

$$\Delta_h(p) = \frac{1}{V_3 T} \sum_k \frac{-4r_0^2 m_0^2}{((p-k)^2 + m_\pi^2)(k^2 + m_\pi^2)^2}, \quad (1)$$

where  $V_3 = L_x L_y L_z$  is the three-volume of the lattice,  $r_0$  is the coupling between the scalar interpolation field and the  $\eta'$  and  $\pi$  [13, 16] or the matrix element  $\langle 0 | \bar{\psi}\psi | \eta'\pi \rangle$ , and  $m_0^2 = 2N_f \chi_t / f_\pi^2$  is the hairpin insertion mass which is related to the topological susceptibility  $\chi_t$  in the pure gauge theory.

The Fourier transform (FT) of the dimensionless  $\Delta_h(p)$  for the case of  $\vec{p} = 0$  gives the following contribution to the scalar meson correlator on the Euclidean lattice

$$G_S(\vec{p} = 0) = FT\{a^2 \Delta_h(\vec{p} = 0)\} = -\frac{r_0^2 m_0^2 N_T}{2N_S^3} \times \sum_{\vec{k}} \frac{(1 + E_\pi t)}{2E_\pi^4} e^{-2E_\pi t} + (t \rightarrow N_T - t), \quad (2)$$

where  $E_\pi = \sqrt{\vec{k}^2 + m_\pi^2}$  and the  $(1 + E_\pi t)$  factor is due to the double pole of the would-be  $\eta'$  ghost propagator in the loop.  $N_S$  and  $N_T$  are the number of lattice points in the spatial and time direction respectively. The result for the more general partially quenched case has been derived in Ref. [16] and the corresponding expression for the would-be  $\eta' - N$  one-loop contribution to the nucleon correlator is derived in the study of Roper and  $S_{11}(1535)$  [11].

We shall use the expression

$$W(1 + E_\pi t)e^{-E_{\eta'\pi} t}, \quad (3)$$

where  $W$  is referred to as the spectral weight in later discussion, to model the fit of each ghost state contribution. Here we allow the energy,  $E_{\eta'\pi}$ , of the interacting  $\eta' - \pi$  to be fitted to the data, but retain the double pole character of the prefactor  $1 + E_\pi t$ . This should be a good approximation when the  $\eta' - \pi$  interaction is weak (N.B. in the large  $N_c$  consideration, the meson-meson interaction is of the order  $1/N_c$ ) so that the prefactor due to the double pole in the would-be  $\eta'$  propagator remains largely valid when

higher orders are included. We have used a similar expression to fit the  $\eta'N$  ghost states in the nucleon and  $S_{11}(1535)$  correlators [11] and found that their spectral weights have the correct 3-volume dependence for the range of quark masses we calculated. Thus, we shall employ this form to fit the  $a_0$  correlator and, as a cross check, will examine if the  $1/E_\pi^4$  dependence in Eq. (2) is borne out from the fit.

We use the above-mentioned SEBM [23] to perform the curve-fitting with the weight  $W$  of Eq. (3) constrained to be negative, to reflect the ghost nature of the state as shown in Fig. 2, and the total energy of the would-be  $\eta'$  and  $\pi$  constrained to be not far from the energy of the two non-interacting pions, i.e.  $2\sqrt{p_n^2 + m_\pi^2}$  with discrete lattice momenta  $p_n = \frac{2\pi n}{L}, n = 0, \pm 1, \dots$ . In the course of studying SEBM [23], we extracted the priors from a subset of the data and applied them in a constrained fit of the rest of the data; we found that the results were very compatible, without detectable bias, with those obtained when the priors were applied to the full data set. In the present work, we extracted the priors from 100 gauge configurations and applied them to a fit of the remaining 200 configurations; we find that the results are very close to those obtained when the priors were applied to the full 300 configurations, except the latter had smaller errors. We shall report the results based on the 300 configurations here. For  $m_\pi \geq 250$  MeV on the  $12^3 \times 28$  lattice, we have been able to fit 4 states with the lowest and the third one being the ghost  $\eta'\pi$  states which are close to the non-interacting pair with each meson at zero momentum, and one unit of lattice momentum ( $p_1$ ), respectively. The second state has a positive weight and is interpreted as the physical  $a_0$  with the usual exponential form  $e^{-Et}$ . We show in Fig. 3 the fits to the  $a_0$  correlators for several low quark masses.

Due to the fact that there are expected to be two to three ghost states below the  $a_0$  on the  $16^3 \times 28$  lattice, we have, unfortunately, not been able to fit all of them to extract the physical  $a_0$  with the SEBM fitting in this case. There are not enough time slices to fit 5 states. Otherwise, we could have compared the spectral weights from the  $12^3 \times 28$  and  $16^3 \times 28$  lattices and checked the expected volume dependence of the one-particle  $a_0$  and two-particle  $\eta' - \pi$  states. However, we could and did compare the ratio of the  $a_0$  correlators  $C_{12}(t)/C_{16}(t)$  between the  $12^3 \times 28$  and the  $16^3 \times 28$  lattices. As was derived in the course of studying pentaquark states [27], the spectral weight of a one-particle state in the point-sink and point-sink correlator is proportional to unity; whereas, that of a weakly interacting two-particle state is proportional to  $1/V_3$ . We show the ratio of the  $a_0$  correlators  $C_{12}(t)/C_{16}(t)$  in Fig. 4 for the cases of  $m_\pi = 764(5)$  MeV and  $m_\pi = 182(8)$  MeV.

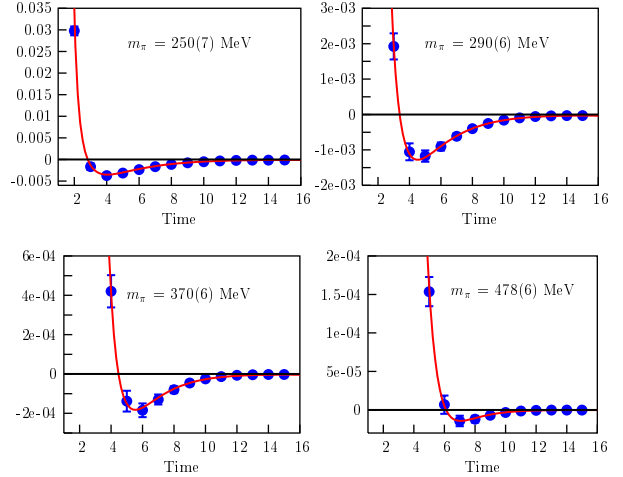


FIG. 3: Fitted  $a_0$  correlators with a low-lying ghost  $\eta'\pi$  state for several quark masses.

In the case of the heavier pion, the ratio of the correlators for the whole time range is close to unity. This reflects the fact that there are no ghost states, so the lowest state is just the scalar  $q\bar{q}$  meson and the ratio of the spectral weights is independent of the volume. On the other hand, the ratio for the  $m_\pi = 182(8)$  MeV case is close to  $[V_3(12)/V_3(16)]^{-1} = 2.37$  for  $t \geq 3$ , indicating that the lowest state is the expected two-particle ghost  $\eta'\pi$  state.

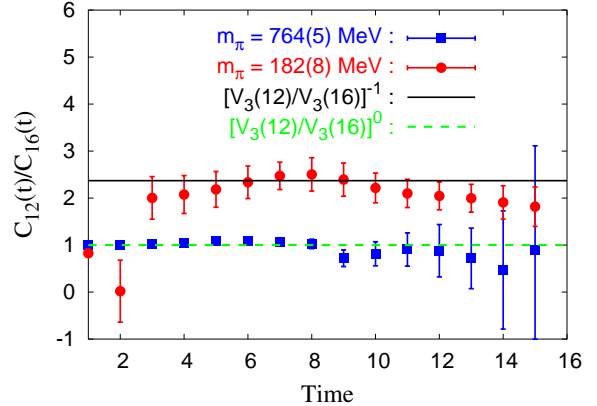


FIG. 4: Ratio of  $a_0$  correlators at  $12^3$  and  $16^3$  lattices for the cases of  $m_\pi = 764(5)$  MeV and  $m_\pi = 182(8)$  MeV. While the expected two-particle ghost  $\eta'\pi$  state shows volume dependence at lower quark mass, one particle  $a_0$  state does not show any volume dependence at higher quark mass.

In addition, we can check the  $1/E_\pi^4$  dependence in the spectral weight  $W$  as suggested in Eq. (2). We adopted the fitting form in Eq. (3) based on the premise that the higher loop diagrams are not important. If the spectral weight indeed exhibits the

$1/E_\pi^4$  dependence, it would lend support for such an assumption. We note that there are two ghost  $\eta'\pi$  states below the physical  $a_0$  on the  $12^3 \times 28$  lattice for pion mass below 250 MeV. In this case, the lowest interacting would-be  $\eta'$  and  $\pi$  scattering state is close to the non-interacting pair with each meson at zero momentum; the second is close to the non-interacting pair with each meson having one unit of lattice momentum, i.e.  $p_1$ . We have been able to fit 4 states in the time window from  $t = 12 - 13$  to  $t = 2$ . The third state has a positive weight and is interpreted as the physical  $a_0$  with the usual exponential form  $e^{-Et}$ . Plotted in the left panel of Fig. 5 is the spectral weight  $W_1$  that we fitted for the lowest ghost  $\eta' - \pi$  state as a function of the pion mass. We see that as the  $m_\pi$  decreases, it is quite singular. We fitted with  $1/E_\pi^4$  from the pion mass from 575 MeV down to 200 MeV. It is found that one can obtain a good fit down to  $m_\pi \sim 270$  MeV. Below  $\sim 270$  MeV, there is a deviation. This is presumably due to the higher order effect. Similarly, we plot the spectral weight  $W_2$  in the right panel in Fig. 5. We see that it is non-zero below  $m_\pi \sim 250$  MeV and its magnitude increases as  $E_\pi$  decreases. However, it does not increase nearly as fast as  $1/E_\pi^4$ . We conjecture that we may not have isolated the second ghost state in our SEBM fit and it may have included higher ghost contribution. Since the second ghost state starts to show up below  $m_\pi = 250$  MeV where the fitted spectral weight  $W_1$  starts to deviate from the expected  $1/m_\pi^4$  behavior, we do not quote results on  $a_0$  below  $m_\pi = 250$  MeV.

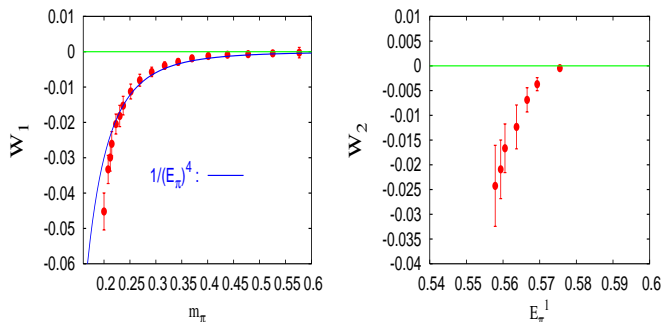


FIG. 5: Fitted spectral weight  $W_1$  for the lowest ghost state (left panel) and  $W_2$  for the second ghost state in the  $a_0$  correlator from the  $12^3 \times 28$  lattice as a function of the pion mass and energy in GeV.

Given the caveats of the ghost state fitting, we interpret the second state from our resultant fit from the  $12^3 \times 28$  lattice which has the ordinary exponential form in time and positive spectral weight to be the physical  $a_0$ . We plot its mass as a function of the corresponding  $m_\pi^2$  in Fig. 6 together with that of  $a_1$  for comparison. The latter does not have

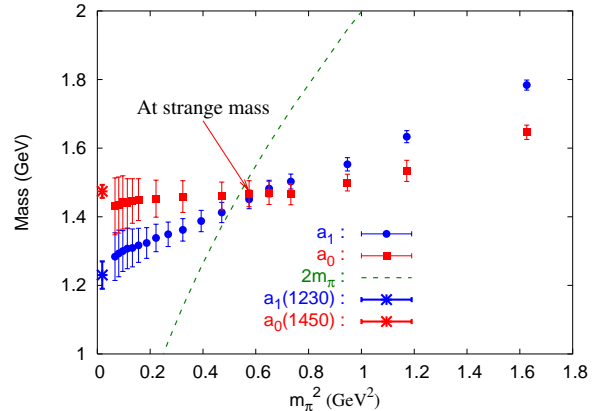


FIG. 6:  $a_0$  and  $a_1$  masses are plotted as a function of  $m_\pi^2$ . Also shown is the two pion mass (dashed line) which becomes lower than  $a_0$  around the strange quark mass region.

ghost state contamination and is thus easier to calculate. We see that above the strange quark mass,  $a_1$  lies higher than  $a_0$  as expected from the quark model of heavy quarks. However, when the quark mass is smaller than that of the strange,  $a_0$  levels off, in contrast to  $a_1$  and the other hadrons that have been calculated on the lattice. This confirms the trend that has been observed in earlier works at higher quark masses [12, 13, 16]. The chirally extrapolated mass  $a_0 = 1.42 \pm 13$  GeV suggests that the meson  $a_0(1450)$  is a  $q\bar{q}$  state. By virtue of the fact that we do not see  $a_0(980)$  which lies lower than  $a_0(1450)$ , we estimate the spectral weight ratio  $\langle 0|\bar{\psi}\psi|a_0(980)\rangle^2/\langle 0|\bar{\psi}\psi|a_0(1450)\rangle^2$  to be less than 0.015 from the relative error of the correlator in the time window where  $a_0$  is fitted. We also calculated the  $K_0(1430)$  mass with the strange mass fixed at  $ma = 0.26833$  which gives a vector meson mass corresponding to the  $\phi$  mass and the  $u/d$  is extrapolated to the chiral limit. In this case, we also need to fit and remove the ghost  $K\eta'$  states due to the hairpin diagram of the  $u/d$  quark. There is no ghost state due to the  $s$  quark, since according to Fig. 2, no ghost state is seen for quark mass greater than  $1/4$  of that of the strange. As a result, we obtain the  $K_0(1430)$  mass at  $1.41 \pm 0.12$  GeV and the corresponding scalar  $\bar{s}s$  state from the connected insertion to be  $1.46 \pm 0.05$  GeV. Our findings are quite consistent with the experimental fact that  $K_0(1430)$  is basically degenerate with  $a_0(1450)$  despite having one strange quark. This unusual behavior is not understood as far as we know and it serves as a challenge to the existing hadronic models.

It is known that the scale in the quenched approximation is not determined uniquely. We note that if the Sommer scale  $r_0 = 0.5$  fm is used for the

scale, the lattice spacing will be 12% smaller, i.e.  $a = 0.175(3)$  fm. As a result, all the masses determined above will be  $\sim 14\%$  higher in the  $r_0 = 0.5$  fm scale. The same is true with the following calculation of the  $\pi\pi$  state and the tetraquark mesonium.

Since we do not see  $a_0(980)$  in the  $a_0$  correlator with the  $\bar{\psi}\psi$  interpolation field, it leaves room for it to be something other than a  $q\bar{q}$  state, e.g. a  $q^2\bar{q}^2$  state as suggested in model studies. However, it is a challenge to verify it on the lattice due to the complication that there is a threshold  $K\bar{K}$  state nearby (within 10 MeV). Therefore, we shall study the  $\sigma(600)$  first which, if present as a tetraquark mesonium, is several hundred MeV above the  $\pi\pi$  threshold and several hundred MeV below the next  $\pi\pi$  scattering state with momentum close to  $p_1$ . This is so, provided that the pion mass is lower than  $\sim 250$  MeV, and it may present the best hope of detecting such a state without the worry of entanglement with the collateral two-meson scattering states. Since the lowest pion mass in our case is 182 MeV, we are in a position to examine it.

### III. $\sigma(600)$ MESON

The  $\sigma$  meson was first postulated by M.H. Johnson and E. Teller as a classical field to explain the saturation properties and binding energies of nuclei; they estimated a mass  $\sim 500$  MeV from the surface energy [32]. It has been suggested that the  $\sigma$  is partially responsible for the enhancement of the  $\Delta I = 1/2$  decay in  $K \rightarrow \pi\pi$  [33]. Although it has been put back in the particle data table on account of the  $D^+ \rightarrow \pi^-\pi^+\pi^+$  experiment [34], its experimental existence is still not fully settled due to the complication that its large width is as large as its mass. Recent dispersion analysis [35] using the Roy equation has produced a resonance pole in  $\pi\pi$  scattering with high precision. The mass is given as  $441_{-8}^{+16}$  MeV with a width of  $544_{-25}^{+18}$  MeV. Lattice QCD, in principle, is capable of resolving the issue about its existence.

Resonance can be viewed as a mixture of a bound state and the scattering states in the usual potential model description of scattering and resonance. In a coupled channel approach, one can couple a bound state in the continuum with the scattering states via a coupling potential resulting in a bound state leaking to the continuum with a shift in mass and acquiring a width. On a hypercubic lattice with periodic boundary conditions, the available momenta are  $p_n = n\frac{2\pi}{La}$ ,  $n = 0, \pm 1, \pm 2 \dots$  and therefore the one- and two-meson spectra for a certain quantum number are discrete. Imagine one considers a very large box where the two-meson spectrum has

closely-spaced levels. When one looks at the spectral weights of the correlator in the channel with a specific quantum number, there will be envelopes of states with enhanced spectral weights which are the result of the mixture of a bound state and the nearby scattering states. They are the finite box representation of the resonances in the continuum. The “width” of the structure would reflect how far apart in energy the mixing takes place. If we start to decrease the size of the box, the spectrum is going to be less dense and states are further apart from each other. The number of states under the envelope diminishes. When the box is small enough so that the scattering states are spaced enough apart that none is expected to lie under the envelope, then only the bound state remains and thus can be identified as such. By being “far enough apart” we mean that we can define the separation of the scattering states  $\Delta$  to be several times greater than the width  $\Gamma$  of the structure, i.e.  $\Delta \gg \Gamma$ . In this case, the bound state and the scattering states are not mixed and they will each have a different volume dependence in their spectral weights. Comparing the spectral weights of the same unmixed state in two lattice volumes is an effective way of revealing the one- or two-particle nature of the state [11, 27] when the interpolation field projects to both the bound and scattering spectra in the correlator with a definite quantum number. This is our approach of identifying, through the volume study of their spectral weights, both a bound tetraquark state (the  $\sigma$ ) and a two-pion scattering state which are reasonably well separated and unmixed.

Experimentally,  $\sigma$  is a very broad state with a width of 544 MeV according to the recent dispersion analysis [35]. It is natural to ask if it is ever possible to delineate it with a lattice calculation in Euclidean space. To answer this, we shall reverse the above discussion on the existence of the bound state. Suppose one finds a bound state in addition to the scattering states which are outside the “width” of the state at a relatively small volume. To gain information about the scattering phase shift and hence the real width, we now increase the box size. As the box size is increased, the energies of the scattering states will be lowered since the value of the discrete momenta decreases. When the scattering state above the bound state is lowered to within the range of the “width”, it mixes with the bound state (this actually defines the range of the width) and the two states avoid the level crossing. From the energy of the scattering state one can deduce the scattering phase shift using the Lüscher formula [36, 37, 38, 39, 40]. This is valid for elastic scattering irrespective of how broad the state is. This is studied in detail in a 2-D lattice model [38] and a spin model [39] which illustrate

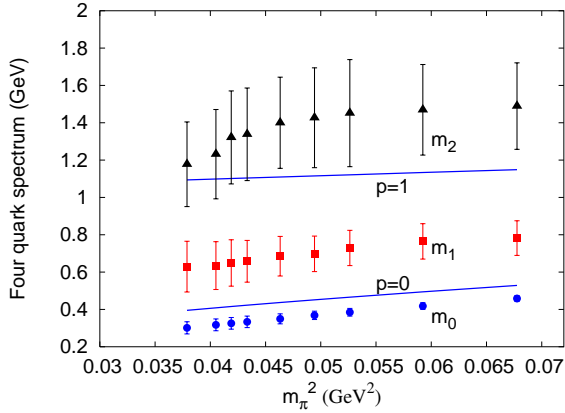


FIG. 7: The lowest three states from the scalar tetraquark correlator as a function of  $m_\pi^2$  for  $m_\pi$  from 182 MeV to 250 MeV on the  $12^3 \times 28$  lattice. The solid lines indicate the energies of the two lowest non-interacting pions in S-wave with lattice momenta  $p_0 = 0$  and  $p_1 = 2\pi/La$ .

how the scattering state mixes with the bound state and gives rise to the phase shift as the volume is increased. In a sense, by varying the lattice volume, hence the momentum, one can use a scattering state to mix with the bound state and scan the spectrum to obtain the phase shift and therefore the width of the resonance. The information of the width can also be obtained by determining how far apart in energy the scattering and bound state start to avoid the level crossing.

In the present manuscript, we are only concerned about the existence of  $\sigma$  and will leave the study of its width to the future. In this vein, we have chosen the lattice size such that the two lowest  $\pi\pi$  scattering states are expected to be more than half of the experimental width, i.e. 272 MeV, away from the expected  $\sigma$  mass at  $\sim 600$  MeV. If this expected result is borne out, we can use the volume test to discern the particle content of the states and thereby distinguish the bound  $\sigma$  from the two-pion scattering states. This is basically our strategy to seek the existence of  $\sigma$ .

To confirm the existence of  $\sigma(600)$  beyond doubt, one needs to identify both the tetraquark mesonium and the collateral  $\pi\pi$  scattering states. Secondly, one needs to work on a lattice where the scattering states and the bound state are well separated (e.g. further apart than half of the width of the “would-be” resonance) to avoid admixture; this is in order to discern the nature of these states separately to make sure that  $\sigma$  is indeed a one-particle state, not a two-particle scattering state. To this end, we used the adaptive Bayes curve-fitting method [23] as described above to fit the ground state and the excited states of the tetraquark correlator with a lo-

cal interpolation operator  $\bar{\psi}\gamma_5\psi\bar{\psi}\gamma_5\psi$  for both the source and the sink. We note that it does not matter what interpolation field one uses for the calculation, as long as it has overlap with the states of the corresponding quantum number. Being local, the pseudoscalar-pseudoscalar operator that we adopt will have vector-vector, scalar-scalar,  $\dots$  components after Fierz transform. This aspect has been discussed in the calculation of the exotic  $I = 2$   $\rho\rho$  states [41]. It is also shown in the pentaquark study that different interpolation fields are related through Fierz transform [27] and the masses from these interpolation fields were verified to be the same in a lattice calculation [42]. Unlike in the  $a_0$  correlator, there are no  $\eta'\pi$  ghost states to worry about in this tetraquark channel. As in Ref. [20], we consider only the connected insertion, not the single and double annihilation insertions. They are likely to preferentially project to the higher  $q\bar{q}$  and glueball states [20]. To verify this, we use two point sources at  $t = 0$  and  $t = 8$  and a zero-momentum wall source in the Coulomb gauge at  $t = 14$  to calculate the disconnected-insertion correlator at time separations  $t - t_0 = 0, 6$ , and 14 and found that they are an order of magnitude smaller than the corresponding connected-insertion correlator. This shows that the annihilation diagrams are not likely to change the results of the connected insertion qualitatively. We present our results on the  $12^3 \times 28$  lattice in Fig. 7 as a function of  $m_\pi^2$  for the pion mass range from 182 MeV to 250 MeV. We have fitted three states so that we can trust the results of the two lower ones. The lowest one is about 100(20) to 60(10) MeV below the  $\pi\pi$  threshold. This is most likely the interacting state of two pions with energy close to and below that of two non-interacting pions at rest, since the interaction is attractive in the  $I = 0$  channel. It is shown that the energy shift of two interacting particles in a finite box can be related to the infinite volume scattering length below the inelastic threshold in a systematic  $1/L$  expansion [36]. In particular, for two spinless bosons with mass  $m$  at rest, one has

$$\Delta E = E - 2m = -\frac{4\pi a_0}{mL^3} \left( 1 + c_1 \frac{a_0}{L} + c_2 \left( \frac{a_0}{L} \right)^2 \right) \quad (4)$$

where  $c_1 = -2.873$  and  $c_2 = 6.3752$  from one-loop calculation [36]. However, it is pointed out [43] that there are would-be  $\eta'$  hairpin diagram contributions at the one-loop order for  $\pi\pi$  scattering which spoils the relation between  $\Delta E$  and the scattering length  $a_0$  in Eq. (4). It has  $L^0$  and  $L^2$  terms in the  $I = 0$  channel in addition to the leading  $1/L^3$  term in Eq. (4). Since our calculation is done in the quenched approximation, using the full QCD one-loop chiral perturbation formula [36] to extract the scattering length of  $\pi\pi$  scattering from the energy

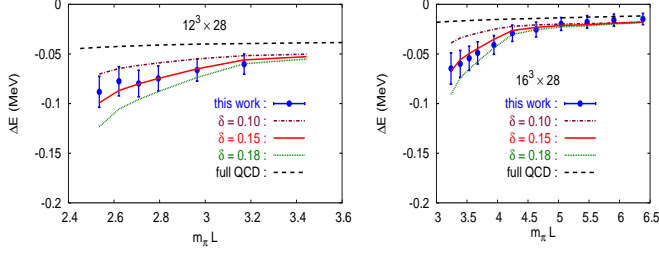


FIG. 8: The calculated energy shift of the lowest  $I = 0$   $\pi\pi$  state  $\Delta E$  as a function of  $m_\pi L$  for the  $12^3 \times 28$  lattice (left panel) and the  $16^3 \times 28$  lattice (right panel). The lines labeled with  $\delta$  indicate the quenched one-loop chiral perturbation results for  $\delta = 0.10, 0.15$  and  $0.18$ . The one-loop full QCD chiral perturbation prediction is also given for comparison.

shift in the finite box channel is not applicable. We shall, instead, compare our results to that derived in quenched chiral perturbation theory. The quenched one-loop  $\pi\pi$  scattering energy shift in the finite box which includes the hairpin diagrams has been derived [43]. The energy shift is

$$\Delta E = E - 2m_\pi = \Delta E^{\text{tree}} + \Delta E^{\text{one-loop}} \quad (5)$$

where the tree-level result for the  $I = 0$  channel is

$$\Delta E^{\text{tree}} = \frac{-7}{4f_\pi^2 L^3}, \quad (6)$$

with  $f_\pi = 132$  MeV at the physical pion mass and the one-loop result is given [43] as

$$\Delta E^{\text{one-loop}} = m_\pi \left[ B_0(m_\pi L) \delta^2 + A_0(m_\pi L) \delta \epsilon + O\left(\frac{\epsilon^2}{(m_\pi L)^3}\right) \right], \quad (7)$$

where

$$\delta \equiv \frac{m_0^2/3}{8\pi^2 f_\pi^2}, \quad \epsilon \equiv \frac{m_\pi^2}{16\pi^2 f_\pi^2}. \quad (8)$$

We interpolate  $B_0(m_\pi L)$  and  $A_0(m_\pi L)$  listed in Ref. [43] for the range of  $m_\pi L$  appropriate for our calculation on the  $12^3 \times 28$  and  $16^3 \times 28$  lattices and plot  $\Delta E$  for  $\delta = 0.10, 0.15$  and  $0.18$  which cover the range of  $\delta$  corresponding to the Witten-Veneziano formula for the  $\eta'$  mass and from the study of quenched chiral log in the pseudoscalar meson masses [29]. The results are presented in Fig. 8 together with our data on the  $12^3 \times 28$  lattice (left panel) and the  $16^3 \times 28$  lattice (right panel) from the lowest state in our calculation which we believe is the two-pion scattering state. We see that our data are

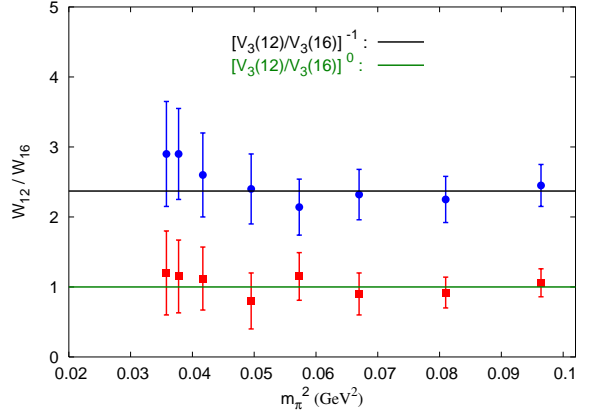


FIG. 9: Spectral weight ratio  $W_{12}/W_{16}$  as a function of  $m_\pi^2$  for the lowest state (filled circle in Fig. 7) and the next lowest state (filled square in Fig. 7).

reasonably consistent with the one-loop quenched chiral perturbation calculation [43] for the range of  $\delta$ , i.e. from 0.10 to 0.18, especially for  $m_\pi L \geq 2.8$  for the  $12^3 \times 28$  lattice and  $m_\pi L \geq 3.5$  for the  $16^3 \times 28$  lattice. This is true despite of the fact that we have not included the disconnected insertion in our calculation. This is consistent with our earlier finding that the disconnected correlator is about an order of magnitude smaller than the connected one at several time separations.

We note that the tree-level energy shift in Eq. (6) is the same in quenched and full QCD. If the energy shift from the loop is small compared to the tree result in both the quenched and full QCD, then the quenched energy shift in Eq. (5) would agree with the full QCD case in Eq. (4). To this end, we plot the energy shift from Eq. (4) with the scattering length  $a_0^{I=0} = \frac{7m_\pi}{16\pi f_\pi^2}$  from the tree-level in Fig. 8 and find that it is about a factor of two to three smaller than our data in the low  $m_\pi L$  region. This shows that the loop contribution in the quenched case is enhanced compared to that in full QCD and not small compared to the tree part and thus one cannot apply the full QCD relation in Eq. (4) to obtain the scattering length. One can only compare the energy shift to that of the quenched chiral perturbation theory as was done in the last paragraph.

The third state in Fig. 7 with a large error bar is about 1 GeV above the lowest state. The fact that it is higher than the energy of the non-interacting two-pion state (each pion with momentum  $p_1 = 524$  MeV), as indicated by the higher solid line, is an indication that the highest fitted state is always higher than the true state as it inevitably includes the unfitted higher states and hence cannot be taken as a good signal for a definite state.

One interesting aspect of the spectrum is that



there is an extra state between the lowest  $\pi\pi$  scattering state and the third state which presumably encompasses the higher scattering states. It has a sizable spectral weight, as large as that of the lower  $\pi\pi$  scattering state. The mass is around 600 MeV. It is tantalizing to identify it with  $\sigma(600)$ . To verify this, we study the volume dependence of the spectral weight of these states. It was advocated in the study of the Roper resonance, the pentaquark, and the ghost state [11, 27] that one efficient way of distinguishing a one-particle state from a two-particle scattering state in a finite box is to study the volume dependence of its spectral weight. From the normalization factor of  $1/\sqrt{V_3}$  for a particle in a box and the way the correlator is constructed, i.e. with a point source and a zero-momentum sink, the spectral weight of a one-particle state does not explicitly depend on volume; whereas, the spectral weight of a weakly interacting two-particle state has an explicit  $1/V_3$  dependence [27]. This is true when the one particle state is reasonably separated from the scattering states so that the mixing of the two states is not strong enough to spoil the characteristic volume dependence of their respective spectral weights. Since we have two lattices with sizes  $12^3 \times 28$  and  $16^3 \times 28$ , the spectral weight ratio for a two-particle state should be  $W_{12}/W_{16} = V_3(16)/V_3(12) = 16^3/12^3 = 2.37$ . Plotted in Fig. 9 are the ratios of the spectral weights for the lowest state in Fig. 7 and the first excited state around 600 MeV. We see that the spectral weight ratio  $W_{12}/W_{16}$  for the lowest state clusters around 2.37, confirming our speculation that it is the interacting two pion state. On the other hand, the spectral weight ratio  $W_{12}/W_{16}$  of the excited state near 600 MeV turns out to be consistent with unity. This suggests that this state is a one-particle state, not a  $\pi\pi$  scattering state, and strongly supports the identification of it to be the  $\sigma(600)$ . Furthermore, by virtue of the fact that the ratios of spectral weights of these two low-lying states are consistent with unity and  $V_3(16)/V_3(12)$ , it suggests that the mixing of the two states, if any, is small. In other words, the two states with an energy separation of  $\sim 300$  MeV are reasonably well separated compared to half of the decay width of  $\sigma(600)$ . Extrapolated to the chiral limit, the mass of the one-particle state is  $540 \pm 170$  MeV.

There have been concerns that the zero mode contributions which are finite volume effects may contaminate the results when the volume is small for the quark mass under study. In the case of the chiral condensate, the zero modes can be avoided by doubling the contribution from the chiral sector which does not have zero modes [44]. For the pion mass calculation, the zero modes can be removed by considering the correlator of the pseudoscalar-

pseudoscalar (PP) and scalar-scalar (SS) combination  $\langle PP \rangle - \langle SS \rangle$  [45, 46]. We have studied the zero mode contributions to the pion mass calculation on the same set of lattices used in the present study [29] by comparing the pion mass from the  $\langle PP \rangle$  correlator and the  $\langle PP \rangle - \langle SS \rangle$  correlator and found that there is no difference in the pion masses within errors. We concluded that the volume is large enough for this lattice that the zero mode contribution is less than the error for the range of quark mass studied. In the present study of  $a_0(1450)$ ,  $K_0^*(1430)$  and  $\sigma(600)$ , we don't see any indication of mass divergence for small quark masses. We thus believe that the zero mode contributions are within errors in the connected insertions.

Although lattice study of tetraquark states started some time ago [20, 41, 47, 48], we believe this is the first time that both the one-particle state and its concomitant scattering state are identified and their nature verified through the volume dependence of the spectral weights. Short of such identification, we don't think one is able to rigorously confirm the existence of the tetraquark mesonium.

Finally, we note that the calculation of tetraquark state with the  $\bar{\psi}\gamma_5\psi\bar{\psi}\gamma_5\psi$  interpolation field has first been attempted [20]. It was found that in the  $I = 0$  channel, the ground state is lower than the expected two interacting pion state from chiral perturbation theory and is interpreted as a bound state — a tetraquark mesonium. However, in this analysis the full QCD formula in Eq. (4) was employed which we pointed out earlier is not applicable to quenched calculations. If the quenched chiral perturbation calculation [43], which has a different lattice length dependence, is used one might come to a different conclusion.

#### IV. CONCLUSION

To conclude, we calculated the isovector  $a_0$  with the  $\bar{\psi}\psi$  interpolation field and  $\sigma(600)$  with the tetraquark interpolation field. With the overlap fermion, we have come down in the chiral region with very low pion mass (182(8) MeV) in the quenched approximation. After removing the fitted  $\eta'/\pi$  ghost states, we found the lowest  $a_0$  at  $1.42 \pm 0.13$  GeV and  $K_0^*$  at  $1.41 \pm 0.12$  GeV which are consistent with the experimental  $a_0(1450)$  and  $K_0^*(1430)$  being the  $q\bar{q}$  states and confirms the earlier findings in quenched and partially quenched calculations at higher quark masses. In addition, we have been able to fit the  $I = 0$  scalar tetraquark correlator and have identified, through the volume study of their spectral weights, both the lowest interacting two-pion state and a one-particle state at  $540 \pm 170$  MeV. This sug-

gests that  $\sigma(600)$  does exist as a particle and it is a tetraquark mesonium. This is consistent with the recent dispersion relation analysis of  $\pi\pi$  and  $K\bar{K}$  scattering with the Roy equation which has led to the  $\sigma$  pole at  $441^{+16}_{-8}$  MeV with a width  $\Gamma_\sigma = 544^{+18}_{-25}$  MeV [35]. Further lattice calculations with dynamical fermion in the chiral region with  $m_\pi < 300$  MeV are needed to check these results.

This work is supported by JSA, LLC under U.S. DOE Contract No. DE-AC05-06OR23177 and by DOE grant DE-FG05-84ER40154, and NFSC grants 10575107 and 10675101. We wish to thank G.E. Brown, M. Chanowitz, H.Y. Cheng, M. Golterman, R. Jaffe, C. Liu, M. Lüscher, D.O. Riska, and F. Wilczek for useful discussions.

- 
- [1] R.L. Jaffe, Phys. Rev. **D15**, 267 (1977).  
[2] K.F. Liu and C.W. Wong, Phys. Lett. **B107**, 391 (1981).  
[3] J. Weinstein and N. Isgur, Phys. Rev. Lett. **48**, 659 (1982).  
[4] B.A. Li and K.F. Liu, Phys. Lett. **B188**, 435 (1982); Phys. Rev. **D30**, 613 (1984); Phys. Rev. Lett. **51**, 1510 (1983).  
[5] B.A. Li and K.F. Liu, Phys. Rev. **D28**, 1636 (1983); *ibid.* **D29**, 416 (1984); Phys. Lett. **B134**, 128 (1984).  
[6] See, for example, E.S. Swanson, [hep-ph/0601110].  
[7] T. Barnes, Phys. Lett. **B165**, 434 (1985).  
[8] N.N. Achasov *et al.*, [hep-ph/0605126].  
[9] S. Eidelman *et al.* (Particle Data Group), Phys. Lett. **B592**, 1 (2004), [see the review on scalar mesons].  
[10] K.F. Liu *et al.*, Phys. Rev. **D59** 112001 (1999).  
[11] N. Mathur, Y. Chen, S.J. Dong, T. Draper, I. Horváth, F.X. Lee, K.F. Liu, and J.B. Zhang, Phys. Lett. **B605**, 137 (2005), [hep-ph/0306199].  
[12] L.-J. Lee and D. Weingarten, Phys. Rev. **D61**, 014015 (2000); M. Gockeler *et al.*, Phys. Rev. **D57**, 5562 (1998); S. Kim and S. Ohta, Nucl. Phys. Proc. Suppl. **B53**, 199 (1997); A. Hart, C. McNeile, and C. Michael, Nucl. Phys. Proc. Suppl. **B119**, 266 (2003); T. Burch *et al.*, [arXiv: hep-lat/0601026].  
[13] W. Bardeen, A. Duncan, E. Eichten, N. Isgur, and H. Thacker, Phys. Rev. **D65**, 014509 (2002); W. Bardeen, E. Eichten, and H. Thacker, Phys. Rev. **D69**, 054502 (2004).  
[14] S. Prelovsek, K. Orginos, Nucl. Phys. Proc. Suppl. **119**, 822 (2003), [hep-lat/0209132].  
[15] C. Bernard *et al.*, Phys. Rev. **D64**, 054506 (2001), [hep-lat/0104002].  
[16] S. Prelovsek, C. Dawson, T. Izubuchi, K. Orginos, and A. Soni, Phys. Rev. **D70**, 094503 (2004).  
[17] T. Kunihiro *et al.*, Phys. Rev. **D70**, 034504 (2004).  
[18] E.B. Gregory *et al.*, PoS LAT2005, 027 (2006), [hep-lat/0510066].  
[19] C. McNeile and C. Michael, Phys. Rev. **D74**, 014508 (2006), [hep-lat/0604009].  
[20] M.G. Alford and R.L. Jaffe, Nucl. Phys. **B578**, 367 (2000), [hep-lat/0001023].  
[21] H. Neuberger, Phys. Lett. **B 417**, 141 (1998).  
[22] G. Colangelo, J. Gasser and H. Leutwyler, Nucl. Phys. **B603**, 125 (2001).  
[23] Y. Chen, S.D. Dong, T. Draper, I. Horváth, K.F. Liu, N. Mathur, S. Tamhankar, C. Srinivasan, F.X. Lee, and J.B. Zhang, hep-lat/0405001.  
[24] G.P. Lepage *et al.*, Nucl. Phys. Proc. Suppl. **106**, 12 (2002), [hep-lat/0110175].  
[25] C. Morningstar, Nucl. Phys. Proc. Suppl. **109**, 185 (2002), [hep-lat/0112023].  
[26] Ying Chen, Chuan Liu, Yubin Liu, Jianping Ma, and Jianbo Zhang (CLQCD Collaboration), hep-lat/0701021.  
[27] N. Mathur, F.X. Lee, A. Alexandru, C. Bennhold, Y. Chen, S.J. Dong, T. Draper, I. Horvath, K.F. Liu, S. Tamhankar, and J.B. Zhang, Phys. Rev. **D70**, 074508 (2004), [hep-ph/0406196].  
[28] H.Y. Cheng, C.K. Chua, and K.F. Liu, Phys. Rev. **D74**, 094005 (2006), [hep-ph/0607206].  
[29] Y. Chen, S.J. Dong, T. Draper, I. Horváth, F.X. Lee, K.F. Liu, N. Mathur, and J.B. Zhang, Phys. Rev. **D70**, (2004) 034502.  
[30] M. Golterman, Y. Shamir, and B. Svetitsky, Phys. Rev. **D72**, 034501 (2005), [hep-lat/0503037].  
[31] T. Draper, N. Mathur, J.B. Zhang, A. Alexandru, Y. Chen, S.J. Dong, I. Horváth, F.X. Lee, K.F. Liu, S. Tamhankar, [hep-lat/0607110].  
[32] M.H. Johnson and E. Teller, Phys. Rev. **98**, 783 (1955).  
[33] T.N. Pham, Phys. Rev. **D33**, 1499 (1986).  
[34] E.M. Aitala, Phys. Rev. Lett. **86**, 770 (2001).  
[35] I. Caprini, G. Colangelo and H. Leutwyler, Phys. Rev. Lett. **96**, 132001 (2006), [hep-lat/0512346].  
[36] M. Lüscher, Comm. Math. Phys. **104**, 177 (1986); *ibid* **105**, 153 (1986).  
[37] M. Lüscher, Nucl. Phys. **B354**, 531 (1991); *ibid* **B364**, 237 (1991).  
[38] C.R. Gatttringer and C.B. Lang, Phys. Lett. **B274**, 95 (1992); Nucl. Phys. **B391**, 463 (1993).  
[39] K. Rummukainen and S. Gottlieb, Nucl. Phys. **B450**, 397 (1995).  
[40] B. Pozsgay and Takács, [hep-th/0604022].  
[41] Y. Liang, B.A. Li, K.F. Liu, T. Draper, and R.M. Woloshyn, Nucl. Phys. Proc. Suppl. **17**, 408 (1990).  
[42] K.F. Liu and N. Mathur, Int. J. Mod. Phys. **A21**, 851 (2006), [hep-lat/0510036].  
[43] C. Bernard and M. Golterman, Phys. Rev. **D53**, 476 (1996), [hep-lat/9507004].  
[44] R. Edwards, U.M. Heller, and R. Narayanan Phys. Rev. **D59**, 094510 (1999), [hep-lat/9811030].  
[45] T. Blum *et al.*, Phys. Rev. **D69**, 074502 (2004).  
[46] S.J. Dong, T. Draper, I. Horvath, F.X. Lee, K.F. Liu, and J.B. Zhang, Phys. Rev. **D65**, 054507 (2002), [hep-lat/0108020].

- [47] A.M. Green, C. Michael and J.E. Paton, Nucl. Phys. **A554** (1993) 701; A.M. Green, C. Michael, J.E. Paton and M.E. Sainio, Int. J. Mod. Phys. **E2** (1993) 479; S. Furui, A.M. Green and B. Masud, Nucl. Phys. **A582** (1995) 682; A.M. Green, J. Lukkari-  
nen, P. Pennanen and C. Michael, Phys. Rev. D **53** (1996) 261; P. Pennanen, Phys. Rev. D **55** (1997) 3958.
- [48] T.W. Chiu and T.H. Hsieh, Phys. Rev. **D73**, 094510 (2006); Phys. Lett. **B646**, 95 (2007).